Photochemical & Photobiological Sciences

Accepted Manuscript

This is an *Accepted Manuscript*, which has been through the Royal Society of Chemistry peer review process and has been accepted for publication.

Accepted Manuscripts are published online shortly after acceptance, before technical editing, formatting and proof reading. Using this free service, authors can make their results available to the community, in citable form, before we publish the edited article. We will replace this *Accepted Manuscript* with the edited and formatted *Advance Article* as soon as it is available.

You can find more information about *Accepted Manuscripts* in the Information for Authors.

Please note that technical editing may introduce minor changes to the text and/or graphics, which may alter content. The journal's standard Terms & Conditions and the Ethical guidelines still apply. In no event shall the Royal Society of Chemistry be held responsible for any errors or omissions in this *Accepted Manuscript* or any consequences arising from the use of any information it contains.

ROYAL SOCIETY OF CHEMISTRY

www.rsc.org/pps

Graphical abstract

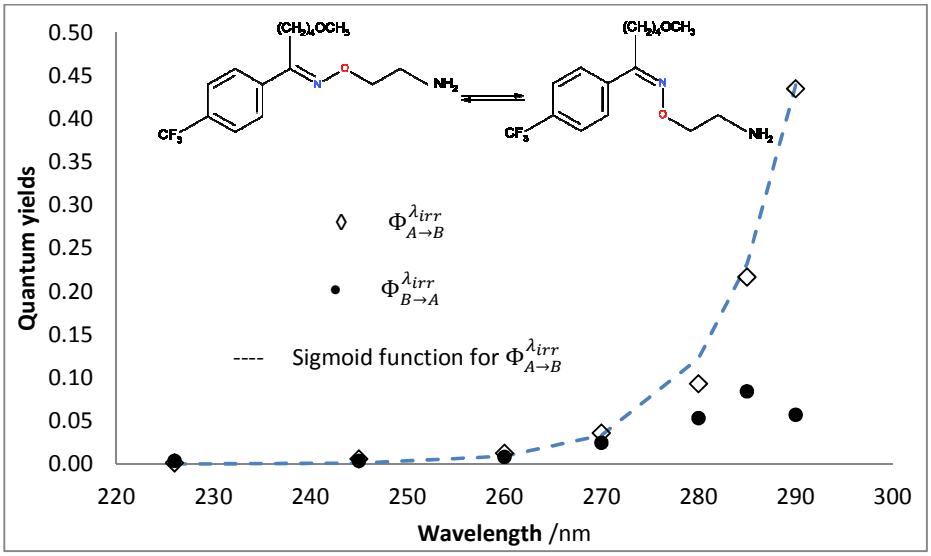

Wavelength–dependent forward ($\Phi_{A\rightarrow B}^{\lambda_{irr}}$) and reverse ($\Phi_{B\rightarrow A}^{\lambda_{irr}}$) *Fluvo* quantum yields.

Quantitative assessment of photostability and photostabilisation of Fluvoxamine and its design for actinomery.

Mounir Maafi*, Wassila Maafi

Leicester School of Pharmacy, De Montfort University, The Gateway, Leicester LE1 9BH, UK

*Corresponding Author: e–mail: mmaafi@dmu.ac.uk (m maafi);

Abstract

Despite the numerous concerns that have been raised in relation to considering 0^{th}, 1^{st} and 2^{nd}–order kinetic treatments for drugs' photodegradation characterisation and assessments, yet they still are employed, as the only tool available for these types of studies. The recently developed Φ–order kinetic models have opened new perspectives in the treatment of photoreaction kinetics that stands as the best known alternative to the classical approach. The Φ–order kinetics have been applied here to Fluvoxamine (Fluvo) with the aim to set out a detailed and comprehensive procedure able to rationalise photodegradation/photostability of drugs and propose a platform for photosafety studies. Our results prove that drugs' quantum yields ($0.0016 < \Phi_{Fluvo}^{\lambda_{irr}} < 0.43$) should *a priori* be considered wavelength–dependent, their photostabilisation (up to 75% for Fluvo) by means of absorption competitors could explicitly be related to a decrease of the photokinetic factor, and photoreversible drugs can be developed into efficient actinometers (as Fluvoxamine in the 260–290 nm range). A pseudo–rate–constant factor was proposed as a descriptive parameter, circumventing the limitations of overall rate–constants and allowing comparison between drugs' kinetic data obtained in different conditions.

Keywords:

Photodegradation, photokinetics, Fluvoxamine, actinometry, photosafety, photostabilization.

1. INTRODUCTION

A vast number of drugs have been shown to be adversely affected by light both *in vivo* and *in vitro*.[1-4] Consequently, several studies have been devoted to the elucidation of the mechanisms, photo–products, kinetics and photoprotection strategies of such photodegradation reactions.[5-7] Thus far, the kinetic analysis of these reactions has relied solely on the classical thermal zeroth–, first– and second–order reaction models.[5,6] Nevertheless, despite the fact that it soon became evident that such treatment strategies are not suited for photochemical reactions, they continued to be employed, mainly due to the lack of more adequate alternative treatments, procedures and methods. This situation has considerably limited the scope and reliability of drugs' photodegradation and photostabilisation studies. The efforts that may have been devoted to proposing integrated rate–laws for photokinetic data that truly reflect the evolution of photoreactions are very scarce in the literature and predominantly based on approximations. This *status quo* is due to the tedious and mostly unsolvable mathematical hurdles encountered during integration of photoreactions' differential equations.[8,9] Recently, an approach was proposed whereby semi–empirical rate–law model equations could be developed for photodegradation reactions. It has also been shown that such photoreactions obeyed a Φ–order kinetics, with a quite different formulation to the classical ones.[10,11] The Φ–order kinetic models, which proved to successfully describe drugs' photoreactions undergoing unimolecular or reversible isomerization,[10,12] have considerably facilitated photostability investigations.

Fluvo is a selective serotonin (5–hydroxytryptamine, 5–HT) neuronal re–uptake inhibitor (SSRI) used in the treatment of depression and anxiety.[13-15] It has a few side effects[16] and little or no anticholinergic effect which makes it a much less hazardous drug than other antidepressants especially in overdose quantities.[17,18]

While this molecule is stable to hydrolysis,[19] it undergoes reversible geometric photoisomerism under UV irradiation around the oxime linker group, Scheme 1.[20] The occurrence of only one photoproduct (*Z–Fluvo*) was evidenced for the photodegradation of *E–Fluvo*.[20,21] While a number of pharmacological experiments have failed to link the *Z*–isomer to any phototoxicity, it was nonetheless found to be a 150–times less potent than its *E*–counterpart when tested on cortical synaptosomes.[19,22] UVB irradiation was deemed responsible for *E–Fluvo* isomerisation and thus interaction of this type of radiation with *Fluvo* and subsequent isomerisation could occur even *in vivo* since UVB is able to reach blood vessels in the dermis.[20] Incidentally, the occurrence of SSRIs in aquatic environments, wastewater and even drinking water sources has also been reported.[23] As such, the study of the photodegradation kinetics of these drugs becomes important not only from a pharmacological but also from an environmental point of view.

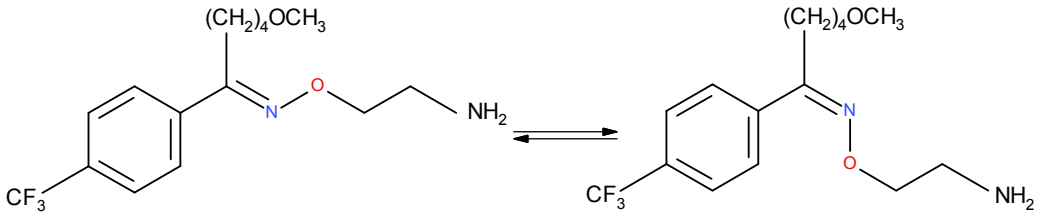

Scheme 1: *E/Z* (Anti/Syn) reversible photoisomerism of *Fluvo* upon exposure to UV–irradiation.

Very little is known on the photodegradation kinetics of *Fluvo*.[20,21] Its photodegradation was attributed the pseudo–first order kinetics under fluorescent lamp irradiation (with a beam's bandwidth of 110 nm, ranging between 290–400 nm with a maximum emission at 312 nm)[21] and differing half–life times were recorded depending on the spectral output of the lamps used for irradiation.[20] Relatively low quantum yield values of *Fluvo* photodegradation in different aqueous media (1.87×10^{-3} to 8.55×10^{-3}) have been

recorded for the experiment using irradiation light from fluorescent lamps.[21] Nevertheless, to the best of our knowledge, neither quantum yield determination for the individual forward ($E \rightarrow Z$) and reverse ($Z \rightarrow E$) reactions nor experiments involving UVB radiation have, thus far, been attempted.

In this paper, the issues highlighted above have been addressed together with a quantification of the effect of light absorbing competitors and *Fluvo* suitability for actinometry.

2. Materials and methods

2.a Materials

Fluvoxamine maleate, 2–{[(E)–{5–Methoxy–1–[4–(trifluoromethyl)phenyl] pentylidene} amino]oxy}ethanamine (*E–Fluvo*), glacial acetic acid and Spectrophotometric grade acetonitrile were purchased from Sigma–Aldrich. Double distilled water was used as the solvent.

2.b Monochromatic continuous irradiation

For irradiation experiments, a Ushio 1000 W xenon arc–lamp light source housed in a housing shell model A6000 and powered by a power supply model LPS–1200, was used. This setting was cooled by tap water circulation through a pipe system. The lamp housing was connected to a monochromator model 101 that allows the selection of specific irradiation wavelenghths since it consists of a special f/2.5 monochromator with a 1200 groove/mm at 300 nm blaze grating. The excitation beam was guided through an optical fibre to impinge from the top of the sample cuvette i.e. the excitation and the analysis light beams were perpendicular to each other. The set up (lamp, lamp housing and monochromator) was manufactured by Photon Technology International Corporation.

2.c The monitoring system

A diode array spectrophotometer (Agilent 8453) was used to measure the various absorption spectra and kinetic profiles for the irradiation and calibration experiments. This spectrophotometer was equipped with a 1–cm cuvette sample holder and a Peltier system model Agilent 8453 for temperature control. As such, the sample was kept at 22°C, stirred

continuously during the experiment, and completely shielded from ambient light. The spectrophotometer was monitored by an Agilent 8453 Chemstation kinetics–software.

A Radiant Power/Energy meter model 70260 was used to measure the radiant power of the incident excitation beams.

2.d Kinetic data treatment

In order to carry out non–linear fittings and to determine best–fit curves, a Levenberg–Marquardt iterative program within the Origin 6.0 software was used.

2.e HPLC measurements

The HPLC system consisted of a reversed–phase Jupiter 5µ C–18 300A Phenomenex (250 x 4.60 mm) column equipped with Perkin Elmer Series 200 pump, UV/Vis detector, vacuum degasser and a Perkin Elmer type Chromatography Interface 600 series Link linked to a computer system.

The mobile phase consisted of 60 % double distilled water adjusted to pH 4.8 with glacial acetic acid and 40 % acetonitrile. A flow rate of 1.5 ml/min and an injection loop of 20 µl were used. The detector wavelength was set at 245 nm. Retention times of 10 and 8.32 min were recorded for E and Z isomers, respectively.

2.f Fluvo solutions

A 2.88 x 10^{-4} M stock solution of *Fluvo* in water was prepared by weighing the solid. The flask was protected from light by aluminium foil wrapping and was kept in the fridge. The

stock solution was diluted to prepare fresh analytical solutions (*ca.* 2 x 10^{-6} M) for analysis of irradiation experiments performed at various wavelengths.

For actinometric studies, *Fluvo* solutions of the same concentrations (*ca.* 2.9 x 10^{-6} M) were exposed to specific wavelengths irradiations (260, 270, 280, 285 and 290 nm) using a series of different intensities for each wavelength. The kinetic traces were observed at the observation wavelength $l_{\lambda_{obs}}$= 245 nm and subsequently fitted with the Φ–order equations.

Experiments were conducted at least in triplicates.

3. RESULTS AND DISCUSSION

3.a The Mathematical background

3.a.1 *Φ–Order kinetics for non–isosbestic irradiation*

The kinetic data of direct unimolecular photoreactions and photoreversible dimolecular phototransformations, collected at non–isosbestic and monochromatic irradiation at constant temperature, have recently been shown to obey Φ–order kinetics.[8,10-12] Φ–order kinetics is much more suitable to describe photoreactions than the classical treatments proposed for zeroth–, first– and second–order thermal reactions. Even though ubiquitous, the treatment of photokinetics on the basis of the latter classical reaction orders is unreliable, for at least three main drawbacks inherently linked to this approach. Firstly, the differential equations of photoreactions are generally different from and not possibly integrated in closed–forms as is the case for thermal reactions of 0^{th}–, 1^{st}–or 2^{nd}– order. This means that using such classical orders' treatments for the quantitative investigation of photoreactions must be considered as a mere approximation. Secondly, literature data have reported that the classical approach may lead to a confusion about the reaction order that should be attributed to the photodegradation reaction at hand given that the kinetic data of a given reaction (generally up to half–life time) can well be fitted by the equations corresponding to two different reaction orders (most commonly 0^{th}– and 1^{st}–order). Thirdly, the rate–constant values determined from the experimental data of photodegradation cannot be analytically linked to the experimental conditions and/or reaction attributes. This has made it difficult to compare such rate constants between compounds and/or laboratories.

In this context, the approach adopted to develop the equations of Φ–order kinetics offers a more robust mathematical framework to investigate photoreactions. The model equation, a logarithmic expression involving a time–dependent exponential term, for

unimolecular photoreactions where only the initial species absorbs, have been derived through closed–form integration.[8] This model equation has represented the basis to develop the semi–empirical model equations for both the unimolecular photoreaction where both initial species and photoproduct absorb, and photoreversible reactions. They have been optimised by studying simulated photoreaction traces obtained by numerical Runge–Kutta integration methods.[10,11] These traces, calculated for a wide range of experimental conditions for unimolecular[10] and reversible photoreactions,[11] served for referencing the reliability and validation of the proposed semi–empirical integrated rate–laws.

A unique set of general equations (Eqs. 1a,b) can be derived for photochemical reactions involving two species, the initial molecule, A, and its photoproduct, B, whose transformations might be achieved by one ($A \rightarrow B$) or two ($A \rightleftharpoons B$) photochemical steps, each one characterised by a specific photoreaction quantum yield (Φ_{AB} and Φ_{BA}). Such systems are labelled as AB(1Φ) and AB(2Φ), respectively. Hence, if assumed that the concentration of the excited state is negligible during the progress of the photoreaction while the reaction medium is concomitantly maintained at a constant temperature, homogeneously stirred, and continuously irradiated with a monochromatic beam (with the latter beam's non–isosbestic wavelength (λ_{irr}) correspond to a spectral region where species A and B absorb different amounts of light (P), i.e., the absorption coefficients (ε) of the species are different and might have non–zero values ($\varepsilon_A^{\lambda_{irr}} \neq \varepsilon_B^{\lambda_{irr}} \neq 0$)), then in these conditions, the concentration profiles, $C_A\,(t)$ and $C_B\,(t)$, are dependent on the species absorption coefficients, and given by

$$C_A\ (t) = C_A\ (\infty) + \frac{Log\left[1 + \left(10^{\left[\left(\varepsilon_A^{\lambda_{irr}} - \varepsilon_B^{\lambda_{irr}}\right) \times \left(C_A\ (0) - C_A\ (\infty)\right) \times l_{\lambda_{irr}}\right]} - 1\right) \times e^{-k_{A \leftrightharpoons B}^{\lambda_{irr}} \times t}\right]}{\left(\varepsilon_A^{\lambda_{irr}} - \varepsilon_B^{\lambda_{irr}}\right) \times l_{\lambda_{irr}}} \quad (1a)$$

195

$$C_B\ (t) = C_B\ (\infty) \times \left(1 - \frac{Log\left[1 + \left(10^{\left[\left(\varepsilon_A^{\lambda_{irr}} - \varepsilon_B^{\lambda_{irr}}\right) \times \left(C_A\ (0) - C_A\ (\infty)\right) \times l_{\lambda_{irr}}\right]} - 1\right) \times e^{-k_{A \leftrightharpoons B}^{\lambda_{irr}} \times t}\right]}{\left(\varepsilon_A^{\lambda_{irr}} - \varepsilon_B^{\lambda_{irr}}\right) \times \left(C_A\ (0) - C_A\ (\infty)\right) \times l_{\lambda_{irr}}}\right) \quad (1b)$$

196 were $k_{A \leftrightharpoons B}^{\lambda_{irr}}$ is the overall reaction rate-constant, and $l_{\lambda_{irr}}$ is the optical path length of the
197 excitation light across the reactive medium.

198 For spectrophotometric monitoring of the reaction's evolution, it is preferable to use
199 the logarithmic integrated rate–law equation describing the variation of the total observed
200 absorption ($A_{tot}^{\lambda_{irr}/\lambda_{obs}}(t)$) with time:[11]

201

$$A_{tot}^{\lambda_{irr}/\lambda_{obs}}(t) = A_{tot}^{\lambda_{irr}/\lambda_{obs}}(\infty) + \frac{A_A^{\lambda_{irr}/\lambda_{obs}}(0) - A_{tot}^{\lambda_{irr}/\lambda_{obs}}(\infty)}{A_A^{\lambda_{irr}/\lambda_{irr}}(0) - A_{tot}^{\lambda_{irr}/\lambda_{irr}}(\infty)} \times \frac{l_{\lambda_{obs}}}{l_{\lambda_{irr}}}\ Log\left[1 + \left(10^{\left[\left(A_A^{\lambda_{irr}/\lambda_{irr}}(0) - A_{tot}^{\lambda_{irr}/\lambda_{irr}}(\infty)\right) \times \frac{l_{\lambda_{irr}}}{l_{\lambda_{obs}}}\right]} - 1\right) \times e^{-k_{A \leftrightharpoons B}^{\lambda_{irr}} \times t}\right] \quad (2)$$

202

203 Eq.2 involves only the cumulative observed absorbances ($A_{tot}^{\lambda_{irr}/\lambda_{obs}}$) of the medium
204 which have been measured under the observation ($l_{\lambda_{obs}}$) and not the excitation ($l_{\lambda_{irr}}$)
205 condition (with $l_{\lambda_{obs}}$ being the optical path length of the monitoring light inside the sample).
206 These optical path lengths ($l_{\lambda_{irr}}$ and $l_{\lambda_{obs}}$) are not necessarily equal for a given experiment,

and the absorbance of the medium in the excitation conditions (i.e. corresponding to a measurement along $l_{\lambda_{irr}}$) may not be directly accessible during the experiment.

The coefficients $A_{tot}^{\lambda_{irr}/\lambda_{obs}}(t)$, $A_{tot}^{\lambda_{irr}/\lambda_{obs}}(0)$, $A_{tot}^{\lambda_{irr}/\lambda_{obs}}(pss)$, $A_{tot}^{\lambda_{irr}/\lambda_{irr}}(0)$ and $A_{tot}^{\lambda_{irr}/\lambda_{irr}}(pss)$ in Eq.2 are the measured (along $l_{\lambda_{obs}}$) total absorbances of the medium respectively recorded at reaction time t, at the initial time (t = 0) and either at the end of the reaction or at the photostationary state (*pss*, where t = ∞). The reaction medium is irradiated at a given irradiation wavelength and simultaneously monitored at either a different observation wavelength ($\lambda_{irr}/\lambda_{obs}$) or at the same wavelength ($\lambda_{irr}/\lambda_{irr}$). It is assumed that the reaction is quantitative and proceeds without by–products.

The analytical expression of the exponential factor, $k_{A\leftrightharpoons B}^{\lambda_{irr}}$, in Eqs.1 and 2 which represents the overall reaction rate–constant, is given by,[11]

$$k_{A\leftrightharpoons B}^{\lambda_{irr}} = \left(\Phi_{A\to B}^{\lambda_{irr}} \times \varepsilon_A^{\lambda_{irr}} + \Phi_{B\to A}^{\lambda_{irr}} \times \varepsilon_B^{\lambda_{irr}}\right) \times l_{\lambda_{irr}} \times F_{\lambda_{irr}}(\infty) \times P_{\lambda_{irr}} = \beta_{\lambda_{irr}} \times P_{\lambda_{irr}} \qquad (3)$$

where $\Phi_{A\to B}^{\lambda_{irr}}$ and $\Phi_{B\to A}^{\lambda_{irr}}$ are the forward and reverse quantum yields of the reaction photochemical steps realised at the irradiation wavelength (λ_{irr}); $P_{\lambda_{irr}}$ is the radiant power (expressed in einstein dm^{-3} s^{-1}); $\beta_{\lambda_{irr}}$ is a proportionality factor, and $F_{\lambda_{irr}}(\infty)$ the time–independent photokinetic factor expressed as:

$$F_{\lambda_{irr}}(\infty) = \frac{1 - 10^{-\left(A_{tot}^{\lambda_{irr}/\lambda_{irr}}(\infty) \times \frac{l_{\lambda_{irr}}}{l_{\lambda_{obs}}}\right)}}{A_{tot}^{\lambda_{irr}/\lambda_{irr}}(\infty) \times \frac{l_{\lambda_{irr}}}{l_{\lambda_{obs}}}} \quad (4)$$

As it has been previously shown,[11] Eq.2 describing the kinetics of AB(2Φ) systems, can also allow retrieving the equations set out for pure unimolecular AB(1Φ) reactions ($\Phi_{B\to A}^{\lambda_{irr}} = 0$), where either (i) only the initial compound absorbs the irradiation light (in these conditions $A_{tot}^{\lambda_{irr}/\lambda_{obs}}(\infty) = 0$ and $F_{\lambda_{irr}}(\infty) = 2.3 \cong Ln(10)$)[8,24] or (ii) both the initial compound and its photoproduct (A and B) absorb light at the irradiation wavelength (which corresponds to complete depletion of species A, and therefore, $F_{\lambda_{irr}}(\infty)$ is calculated using Eq.3 with $A_{tot}^{\lambda_{irr}/\lambda_{obs}}(\infty) = A_B^{\lambda_{irr}/\lambda_{obs}}(\infty) = \varepsilon_B^{\lambda_{irr}} \times l_{\lambda_{irr}} \times C_A\ (0)$).[10]

The differentiation of Eq.2 yields the expression of the initial velocity of the reaction $\left((dA_{tot}/dt)_{t=0} = v_{0\ (mod.)}^{\lambda_{irr}/\lambda_{obs}}\right)$, for the kinetic trace involving the variation of the total absorbance,[11]

$$v_{0\ (mod.)}^{\lambda_{irr}/\lambda_{obs}} = \left(\frac{dA_{tot}^{\lambda_{irr}/\lambda_{obs}}}{dt}\right)_0$$

$$= \frac{A_{tot}^{\lambda_{irr}/\lambda_{obs}}(0) - A_{tot}^{\lambda_{irr}/\lambda_{obs}}(pss)}{A_{tot}^{\lambda_{irr}/\lambda_{irr}}(0) - A_{tot}^{\lambda_{irr}/\lambda_{irr}}(pss)} \times \frac{k_{A\leftrightharpoons B\ (mod.)}^{\lambda_{irr}}}{\frac{l_{\lambda_{irr}}}{l_{\lambda_{obs}}} \times Ln(10)}$$

$$\times \left(10^{\left(A_{tot}^{\lambda_{irr}/\lambda_{irr}}(pss) - A_{tot}^{\lambda_{irr}/\lambda_{irr}}(0)\right) \times \frac{l_{\lambda_{irr}}}{l_{\lambda_{obs}}}} - 1\right) \quad (5)$$

The numerical value of Eq.5, obtained graphically, corresponds to the theoretical expression derived from the differentiation of the reaction,[11] as

$$\upsilon_{0\,(cld.)}^{\lambda_{irr}/\lambda_{obs}} = \left(\varepsilon_B^{\lambda_{obs}} - \varepsilon_A^{\lambda_{obs}}\right) \times l_{\lambda_{obs}} \times \Phi_{A\to B}^{\lambda_{irr}} \times \varepsilon_A^{\lambda_{irr}} \times l_{\lambda_{irr}} \times F_{\lambda_{irr}}(0) \times C_0 \times P_{\lambda_{irr}}$$

$$= \delta_{\lambda_{irr}} \times P_{\lambda_{irr}} \qquad (6)$$

When calculating $\upsilon_{0\,(cld.)}^{\lambda_{irr}/\lambda_{obs}}$, the photokinetic factor $F_{\lambda_{irr}}(t)$ at time t = 0 takes the value of $F_{\lambda_{irr}}(0)$, that is determined using $A_{tot}^{\lambda_{irr}/\lambda_{obs}}(0) = \varepsilon_A^{\lambda_{irr}} \times l_{\lambda_{irr}} \times C_A\,(0)$ in lieu of $A_{tot}^{\lambda_{irr}/\lambda_{obs}}(\infty)$ in Eq.4. $\delta_{\lambda_{irr}}$ is a proportionality factor.

Because Eqs.1 and 2 are semi–empirical, their application has been limited to $F_{\lambda_{irr}}(\infty)$ values higher than 1.2. This condition is easily met by reducing the values of either the initial concentration of species A or the optical path length for irradiation, $l_{\lambda_{irr}}$.[10,11]

3.a.2 *Isosbestic irradiations equations*

In the case where the monochromatic irradiation of the solution is realised at an isosbetic point, $\lambda_{irr} = \lambda_{isos}$ (only a few isosbestic points are usually present on the electronic spectra of AB(2Φ) reactions), the general integrated rate–law of AB reaction systems has been obtained through a closed–from integration,[25] as

$$C_A(t) = C_A(\infty) + \left(C_A(0) - C_A(\infty)\right) \times e^{-k_{A\leftrightharpoons B}^{\lambda_{isos}} \times t} \qquad (7)$$

$$C_B(t) = C_B(\infty) - C_B(\infty) \times e^{-k_{A\leftrightharpoons B}^{\lambda_{isos}} \times t} \qquad (8)$$

with $C_A(\infty)$ and $C_B(\infty)$, the concentrations of the species at either the end of the reaction or *pss* (t = ∞) and $k_{A\leftrightharpoons B}^{\lambda_{isos}}$, the overall rate–constant of the reaction performed at an isosbetic irradiation.

$k_{A\leftrightharpoons B}^{\lambda_{isos}}$ has the same analytical expression as Eq.3 but with λ_{isos} replacing λ_{irr} and the photokinetic factor $F_{\lambda_{isos}}$ used instead of $F_{\lambda_{irr}}(\infty)$. $F_{\lambda_{isos}}$ is calculated using Eq.4 with $A_{tot}^{\lambda_{isos}/\lambda_{isos}}$ instead of $A_{tot}^{\lambda_{irr}/\lambda_{irr}}(\infty)$.

The value of the initial velocity can be obtained graphically and compared to its theoretical expression (Eq.9).

$$v_0^{\lambda_{isos}/\lambda_{isos}} = -k_{A\leftrightharpoons B}^{\lambda_{isos}} \times \left(C_A(0) - C_A(pss)\right) = -\Phi_{A\to B}^{\lambda_{isos}} \times C_A(0) \times \varepsilon_A^{\lambda_{isos}} \times l_{\lambda_{isos}} \times P_{\lambda_{isos}} \times F_{\lambda_{isos}} \quad (9)$$

The monoexponential form of the equations 7 and 8 indicates that isosbestic irradiations induce first–order kinetics for AB(2Φ) reactions. This is primarily due to the fact that when $\lambda_{irr} = \lambda_{isos}$, the photokinetic factor does not vary with reaction time (as the medium absorbance at the irradiation wavelength, λ_{isos}, is time–independent).

3.a.3 *The kinetic elucidation method for AB(2Φ) photoreversible reactions*

If, a priori, we suppose that the quantum yields of the photoreaction are wavelength–dependent (until proven otherwise) and the spectra of the species A and B overlap, then the equations set out above for both isosbetic (Eqs.7 and 8) and non–isosbestic (Eq.1 and 2) irradiations can fit well the AB(2Φ) experimental traces obtained photometrically, however,

the extracted fitting parameters ($k_{A\leftrightarrows B}^{\lambda_{isos}}$ and $v_0^{\lambda_{isos}/\lambda_{obs}}$ or $k_{A\leftrightarrows B}^{\lambda_{irr}}$ and $v_0^{\lambda_{irr}/\lambda_{obs}}$), which represent two equations for each irradiation condition, are not sufficient to work out the three unknowns of the reaction namely, its photochemical quantum yield values and the absorption coefficient, $\varepsilon_B^{\lambda_{irr}}$, (i.e. the electronic spectrum) of the photoproduct, if none of the latter is available prior to the experiment. Solving the kinetics by using only the fitting parameters (irrespective of the number of $\lambda_{irr}/\lambda_{obs}$ traces) leads to a degenerate kinetic solution with inextricable identifiability and/or distinguishability issues.[26]

In order to overcome this situation, we have recently proposed a simple elucidation method for photoreversible reactions that can be implemented in three steps.[26]

Firstly, the reaction quantum yields are determined for an isosbestic irradiation. The variation of the species concentrations during photodegradation, under a monochromatic irradiation at an isosbestic point, is monitored by HPLC. At the given irradiation wavelength (λ_{isos}), the absorption coefficient of the photoproduct is known ($\varepsilon_A^{\lambda_{isos}} = \varepsilon_B^{\lambda_{isos}}$) and therefore, the number of unknowns is only two ($\Phi_{A\to B}^{\lambda_{isos}}$ and $\Phi_{B\to A}^{\lambda_{isos}}$) for this experiment.

Hence, fitting the experimental data with Eqs.7 and 8 provides the numerical values for the reaction initial velocity ($v_0^{\lambda_{isos}}$, Eq. 9) and the reaction overall rate–constant ($k_{A\leftrightarrows B}^{\lambda_{isos}}$). In these conditions, solving the system of two equations ($v_0^{\lambda_{isos}}$ and $k_{A\leftrightarrows B}^{\lambda_{isos}}$), leads to the determination of the absolute values of $\Phi_{A\to B}^{\lambda_{isos}}$ (Eq.10) and $\Phi_{B\to A}^{\lambda_{isos}}$ (Eq.11), as

$$\Phi_{A\to B}^{\lambda_{isos}} = \frac{k_{A\leftrightarrows B}^{\lambda_{isos}}}{\varepsilon_A^{\lambda_{isos}} \times l_{\lambda_{isos}} \times P_{\lambda_{isos}} \times F_{\lambda_{isos}}} \times \frac{\left(C_A(0) - C_A(pss)\right)}{C_A(0)} \qquad (10)$$

$$\Phi_{B\to A}^{\lambda_{isos}} = \frac{k_{A\leftrightharpoons B}^{\lambda_{isos}}}{\varepsilon_A^{\lambda_{isos}} \times l_{\lambda_{isos}} \times P_{\lambda_{isos}} \times F_{\lambda_{isos}}} - \Phi_{A\to B}^{\lambda_{isos}} \quad (11)$$

Both the species pss concentrations and the quantum yields' values, allow determining the equilibrium constant (Eq.12),

$$K_{\leftrightharpoons}^{\lambda_{isos}} = \frac{k_{B\to A}^{\lambda_{isos}}}{k_{A\to B}^{\lambda_{isos}}} = \frac{C_B(pss)}{C_A(pss)} = \frac{\Phi_{A\to B}^{\lambda_{isos}}}{\Phi_{B\to A}^{\lambda_{isos}}} \quad (12)$$

It is worth noticing that $K_{\leftrightharpoons}^{\lambda_{isos}}$ is concentration–independent. This feature finds its importance in the fact that the HPLC experiment that served its determination is usually performed at initial concentrations of species A that are not suitable (too concentrated) for spectrophotometric analyses (which are bound to be realised at lower concentration, specifically, where $F_{\lambda_{irr}}(\infty) > 1.2$ as discussed above).

The reconstruction of the full spectrum of the photoisomer (B), can then be performed at lower concentrations in the second step of the elucidation method. This is achieved from the value of $K_{\leftrightharpoons}^{\lambda_{isos}}$ and the spectrum of the reactive medium recorded at *pss* under the same isosbestic irradiation used for the HPLC experiment ($A_{tot}^{\lambda_{isos}/\lambda_{obs}}(pss)$), as

$$\varepsilon_B^{\lambda_{obs}} = \frac{(K_{\leftrightharpoons}^{\lambda_{isos}}+1)\times A_{tot}^{\lambda_{isos}/\lambda_{obs}}(pss) - \varepsilon_A^{\lambda_{obs}} \times l_{obs} \times C_A(0)}{l_{obs} \times K_{\leftrightharpoons}^{\lambda_{isos}} \times C_A(0)} \quad (13)$$

Therefore, irrespective of the wavelength selected to perform the irradiation, the number of unknowns will constantly be two in total, as the spectrum of the photoproduct (ε_B^{λ}) is fully known.

Hence, in the last step of the method, the quantum yields for each non–isosbestic irradiation wavelength ($\Phi_{A\to B}^{\lambda_{irr}}$ and $\Phi_{B\to A}^{\lambda_{irr}}$) can readily be worked out by using Eq.6 and its numerical value given by Eq.5 (for $\Phi_{A\to B}^{\lambda_{irr}}$, Eq.14) and by rearranging Eq.3 (for $\Phi_{B\to A}^{\lambda_{irr}}$) to give Eq. 15.

$$\Phi_{A\to B}^{\lambda_{irr}} = \frac{v_{0\ (mod.)}^{\lambda_{irr}/\lambda_{obs}}}{\left(\varepsilon_B^{\lambda_{obs}} - \varepsilon_A^{\lambda_{obs}}\right) \times l_{\lambda_{obs}} \times \varepsilon_A^{\lambda_{irr}} \times l_{\lambda_{irr}} \times P_{\lambda_{irr}} \times F_0^{\lambda_{irr}} \times C_0} \qquad (14)$$

$$\Phi_{B\to A}^{\lambda_{irr}} = \frac{k_{A\leftrightharpoons B}^{\lambda_{irr}}}{\varepsilon_A^{\lambda_{irr}} \times l_{\lambda_{irr}} \times P_{\lambda_{irr}} \times F_{\lambda_{irr}}} - \Phi_{A\to B}^{\lambda_{irr}} \qquad (15)$$

3.b Fluvo photoreaction

The native electronic absorption spectrum of *E–Fluvo* isomer (Fig.1) can be divided into two main absorption regions, 200–226 nm (Log(ε)= 4.5) and 226–320 nm (Log(ε)= 4.1). This molecule, thus, absorbs mainly in the UVB region of the spectrum as it is the case for non–conjugated oximes, with the long wavelength absorption transition having a $\pi\rightarrow\pi^*$ character.[27] When exposed to a monochromatic irradiation within that region, the spectrum of the solution decreases in the regions 200–215 nm and 226–285 nm and increases in the alternate regions of 215- 226 nm and 285-320 nm (Fig1). The clearly defined isosbestic

points (at 215, 226 and 285 nm) and the smooth evolution of the spectra indicate that the photoreaction is quantitative and proceeds without by–products. Furthermore, *E–Fluvo* and its photoproduct (*Z–Fluvo*, Scheme 1) share a similar overall spectral shape with a 40 % maximum variation in absorbance observed at *ca.* 245 nm.

3.c Determinaltion of the equilibrium constant at an isosbestic irradiation ($K_{\leftrightharpoons}^{\lambda_{isos}}$)

An *E–Fluvo* aqueous solution was subjected to a 226–nm isosbestic/mononchromatic irradiation and the photoreaction was monitored by HPLC at various time intervals until the *pss* was reached. The concentration profiles of *E*– and *Z–Fluvo* were readily fitted by Eqs.7 and 8 (Fig.2), and the fitting parameter, the rate–constant $k_{A\leftrightharpoons B}^{\lambda_{isos}}$, as well as the *pss* concentrations of the reactive species were determined. Subsequently, the forward (Eq.10) and reverse (Eq.11) quantum yield values as well as the equilibrium constant $K_{A\leftrightharpoons B}^{\lambda_{isos}}$ (Eq.12), could be calculated (Table 1). At λ_{isos} = 226 nm, the initial *E*–isomer is found to be more than twice as photoefficient as its counterpart, as indicated by the value of $K_{\leftrightharpoons}^{\lambda_{isos}}$, which resulted, given that $\varepsilon_A^{\lambda_{isos}} = \varepsilon_B^{\lambda_{isos}}$, in a higher proportion of the *Z*–isomer in the *pss* composition, as it is usually observed for *trans–cis* photoisomerization.[28,29]

Table 1: Overall rate–constant and equilibrium constant for the photodegradation of an aqueous *Fluvo* solution (1.37 x 10^{-4} M) exposed to isosbestic monochromatic irradiation at 226 nm, as monitored by *HPLC*.

λ_{isos} /nm	$A_0^{\lambda_{isos}}$	$C_0^{\lambda_{isos}}$ / M	$l_{\lambda_{isos}}$ / cm	$l_{\lambda_{obs}}$ / cm	$C_A(pss)$ / M	$C_B(pss)$ / M	$P_{\lambda_{isos}}$ /einstein.s^{-1}.dm^{-3}	$k_{A\leftrightharpoons B}^{\lambda_{isos}}$ / s^{-1}	$K_{A\leftrightharpoons B}^{\lambda_{isos}}$
226	2.41	1.37x10^{-4}	1	1	4.07x10^{-5}	9.59x10^{-5}	1.88x10^{-6}	3.83x10^{-4}	2.35

3.d Recovery of the Z–isomer's absorption spectrum

Based on Eq.13, the spectrum of the medium at *pss* and the spectrum of the *E*–isomer, the electronic absorption spectrum (as absorption coefficients' values) of the *Z–isomer* can be fully reconstructed (Fig. 3).

3.e Isomers' quantum yields at non–isosbestic irradiation wavelengths

Once the absorption spectrum of the *Z–isomer* was known, the two remaining system unknowns ($\Phi_{A\to B}^{\lambda_{irr}}$ and $\Phi_{B\to A}^{\lambda_{irr}}$) could then be calculated for any irradiation wavelength using the quantum yield expressions given by Eqs.14 and 15.

Seven monochromatic irradiations (λ_{irr} = 290, 285, 280, 270, 260, 245, and 226 nm) that span the isomers' absorption spectra, were selected in this study. The kinetic traces were recorded at a unique observation wavelength λ_{obs} = 245 nm, that corresponds to the most extensive variation of the absorbance (Figs. 1 and 3). In general, a smooth decrease in absorption over irradiation time was observed eventually reaching a plateau region (Fig. 4), as suggested by HPLC measurements. This represents a typical behaviour of AB(2Φ) systems, which in turn corroborates the mechanism of *Fluvo* photodegradation (Scheme 1). This is also confirmed by the good fitting of the kinetic traces with the model equation, Eq.2, for all non–isosbestic irradiations. Therefore, *Fluvo* photoconversion obeys Φ–order kinetics.

The kinetic parameters determined for *Fluvo* photodegrdation (Table 2), indicate that the overall rate–constant of photoreaction increases with increasing irradiation wavelength (Table 2). However, as has been comprehensively discussed in previous studies,[10-12] $k_{Fluvo}^{\lambda_{irr}}$ dependence on a number of experimental parameters (Eq.3), such as initial concentration and

irradiation intensity, reduces its ability to inform about the intrinsic photoreactivity of the molecule. Therefore, it is mandatory to define, in subsequent steps, the absolute values of the photoreaction quantum yields at the selected wavelengths.

The recommended hypothesis for this type of studies is that the quantum yields of drugs should *a priori* be supposed wavelength dependent and then test the hypothesis experimentally.

Table 2: Quantum yields, overall rate–constant, absorption coefficient and initial velocity values for *Fluvo* photodegradation reactions under various monochromatic irradiations, as determined by the Φ–order kinetics.

λ_{irr} /nm	$A_{Fluvo}^{\lambda_{irr}/245}(0)$	$P_{\lambda_{irr}}$ /einstein. $s^{-1}.dm^{-3}$	$A^{\lambda irr}(pss)$	$k_{A\leftrightharpoons B}^{\lambda_{irr}}$ /s^{-1}	$v_{0\,(mod.)}^{\lambda_{irr}/\lambda_{obs}}$ / s^{-1}	$\varepsilon_A^{\lambda_{irr}}$ / $M^{-1}cm^{-1}$	$\varepsilon_B^{\lambda_{irr}}$ / M^{-1} cm^{-1}	$F^{\lambda_{irr}}(0)$	$\Phi_{A\to B}^{\lambda_{irr}}$	$\Phi_{B\to A}^{\lambda_{irr}}$
226	0.0393	6.09 x 10^{-7}	0.0420	0.000197	-2.20x10^{-6}	14254	13802	2.086	0.00383 ± 0.00003	0.00157 ± 0.00027
245	0.0399	5.86 x 10^{-7}	0.0281	0.000268	-3.09x10^{-6}	13478	8273	2.095	0.00612 ±0.00042	0.0038 ± 0.001331
260	0.0398	4.60 x 10^{-7}	0.0191	0.000380	-4.56 x10^{-6}	10687	4997	2.14	0.0128 ± 0.00064	0.0085 ± 0.00096
270	0.0405	5.21 x 10^{-7}	0.0109	0.000670	-8.31 x10^{-6}	6679	1859	2.19	0.0361 ± 0.00195	0.025 ± 0.0035
280	0.0398	5.51 x 10^{-7}	0.0031	0.000875	-1.28 x10^{-5}	3109	829	2.25	0.0931± 0.00275	0.0535±0.0127
285	0.0400	4.70 x 10^{-7}	0.0031	0.00048	-1.32 x10^{-5}	1774	586	2.27	0.2167 ± 0.0059	0.0844 ± 0.0075
290	0.0402	2.56 x 10^{-7}	0.0028	0.00152	-6.69 x10^{-6}	859	596	2.28	0.4349 ± 0.0205	0.0573 ± 0.0184

It is clearly shown from the results of Table 2 that the forward quantum yield ($\Phi_{A\to B}^{\lambda_{irr}}$) increases with increasing wavelength and was always higher than the reverse quantum yield ($\Phi_{B\to A}^{\lambda_{irr}}$). The most pronounced variation of the quantum yield ratios ($1.4 > \Phi_{A\to B}^{\lambda_{irr}}/\Phi_{B\to A}^{\lambda_{irr}} > 7.6$) is situated in the longest wavelength, 280 to 290 nm, region (ranging between 1.7 and 7.5), whereas, a much more modest change in its values is observed in the region 245-280 nm

386 ($1.4 > \Phi_{A\rightarrow B}^{\lambda_{irr}} / \Phi_{B\rightarrow A}^{\lambda_{irr}} > 1.7$). Furthermore, the evolution of the forward quantum yield values with
387 wavelength has a defined sigmoid pattern (Eq.16, Fig.5).

388

$$\Phi_{A\rightarrow B}^{\lambda_{irr}} = \frac{1}{0.07 + 400 \times e^{-(0.13\times(\boldsymbol{\lambda_{irr}}-250))}} \qquad \text{(Eq. 16)}$$

389

390 This advantageously enables the determination of *E–Fluvo* quantum yield at any desired
391 wavelength using the sigmoid equation (Eq.16).

392 The reverse quantum yield, on the other hand, follows a lower pattern with irradiation
393 wavelength (Fig.5), with a 5.4–fold maximum span of variation for the recorded set of values
394 (whereas 11.4 was recorded for the forward quantum yield). A similar behaviour has been
395 observed for Montelukast.[12] The differing magnitude of photo–efficiencies between *E*– and its *Z*–
396 *Fluvo* isomer might suggest a difference in the excited–state associated with each species. The
397 more pronounced difference between the isomers' quantum yields that was recorded in the longest
398 wavelength region indicates that the excited–sate of lowest energy is much more efficient for *E*–
399 than for *Z–Fluvo.* This finding might suppose a more important contribution of the $n\rightarrow\pi^*$ excited–
400 state in *Fluvo* phototransformation. In any case, the increase of quantum yields with irradiation
401 wavelengths, observed for a number of drugs studied in our team, does not have at present a
402 full/comprehensive interpretation. Overall, such results may illustrate a case where not only the
403 chemical nature, the geometry of the molecule but also the irradiation conditions impact the drugs
404 photochemical behaviour.

405 The oxime group within *E–Fluvo* is found to be twice as photochemically efficient as
406 the ethene bond in the stilbene–like Montelukast ($\Phi_{A\rightarrow B}^{\lambda_{irr}}$ = 0.012–0.18).[12] In both these cases,

as well as for nifedipine,[10] the results show a trend of higher forward quantum yield values for lower–energy excited–states.

In terms of photostability, the photoreversibility has the advantage of limiting the depletion of the initial active ingredient to the amounts recorded at the *pss*, however, the *pss* concentration (Z/E) ratios for *Fluvo* isomers, $C_B^{\lambda_{irr}}(pss)/C_A^{\lambda_{irr}}(pss) = \left(\Phi_{A\to B}^{\lambda_{irr}} \times \varepsilon_A^{\lambda_{irr}}\right)/\left(\Phi_{B\to A}^{\lambda_{irr}} \times \varepsilon_B^{\lambda_{irr}}\right)$, increases with wavelength from 2.5 and reaches a value of 11.3 at 290 nm, which indicates a substantial degradation of the initial species (*E–Fluvo*). In the case of *Fluvo*, this represents a significant decrease in dosage as *Z–Fluvo* is biologically inactive,[20] but could be a major issue if for other drugs the photoproduct is toxic. These results stress out the usefulness and necessity of a full kinetics elucidation of drug photodegradation. They also confirm that reliable conclusions about the photoreactivity of a compound can only be reached when using monochromatic irradiation coupled to a treatment using the Φ–order kinetics. It is then reasonable to suggest that the ICH recommendations would benefit from introducing an element of photostability assessment of the drugs at low concentration in solution. Such data would not only shed light on the photokinetic behaviour and photodegradation parameters of the drug *in vitro* but also may lay down a platform for an understanding of the behaviour of drugs *in vivo*. Indeed, the distribution of the administered drugs in the skin and eyes of the patients occurs mostly at low concentration within biological fluids and tissues.[3,4] Many studies have shown that both topical and systemic drugs can cause different conditions including photosensitivity and dermatoses in all-age patients including newborns.[30-33] Even though an exact number of the drugs concerned has not yet been made available, it is nonetheless possible that a very high proportion of existing and future organic drugs, assuming a conservative hypothesis, absorb in the UVA–UVB ranges (some in the visible).[3,4] These types of radiation traverse through

the skin with UVA wavelengths penetrating deep into the dermis.[3,4,20] Hence, most of drugs can reach the excited–state from which they potentially can subsequently photoreact both in *vitro* and in *vivo*. It has been shown that despite that the absorption spectrum of *Fluvo* ends *ca.* 290 nm (Fig.3), exposing the solution of this drug to UVA–Visible light (simulating day light) also caused its degradation.[21] As for most drugs, the variability/progress of the photodegradation depends also on the intensity of the light and/or the duration of the exposure. In this context, the FDA, EMEA and ICH have issued guidelines on the evaluation of the photosafety of all new systemic and topical pharmaceuticals capable of absorbing within the UVB, UVA or visible regions with absorption coefficients above 1000 $M^{-1}.cm^{-1}$ as well as existing drugs when unaddressed photosafety concerns arise.[34-36] The regulatory authorities and pharmaceutical industries increasingly recognise photo-induced pharmaceutical and cosmetic drugs' reactions.[3,4,37] In addition, the advent of an ever wide spreading phototherapy treatments (including home phototherapy),[38,39] calls for clearer and tighter recommendations for photosafety testing. In this context, testing low concentrated solutions of drugs *in vitro* may arguably benefit the evaluation of the potential and extent of photodegradation that might be undergone by the drug in similar situations *in vivo*. The low concentration studies are also important because the equations of the Φ–order kinetics (Eq.3) show that the rate of photodegradation of drugs increases with decreasing concentration.[10] Such low drug concentrations would mimic *in vivo* conditions as for the latter a maximum substrate concentration was set at 100 μg/ml, in addition to a recommendation to perform several dilutions during the testing procedure.[36] This is justified by the fact that most drugs reach the circulation, body tissues and eyes in significantly smaller amounts to the original given dose. Furthermore, the ICH currently recommends an irradiance dose of approximately 5 J/cm^2 UVA doses for the *in vitro* 3T3 Neutral Red Uptake phototoxicity test (3T3 NRU PT)

to corroborate natural irradiation conditions comparable to those obtained during prolonged outdoor activities on summer days around noon time, in temperate zones and at sea levels.[36]

Therefore, the conditions of the present study reflect well the situation of drugs in the body as small concentrations (*ca*. 1.3 μg/ml) and low radiation power (1-2 J/h/cm^2) are employed. Such studies might be thought as a relevant initial platform, that provide reliable data and valuable information about the inherent photoreactivity of a molecule in solution, to feed the evaluation of drugs' photosafety and photodegradation *in vivo*.

3.f Photostabilisation of Fluvo photodegradation using excipient–dyes

There is an evident lack in the literature of useful methods to quantify photostabilisation of drugs. The Q1b document[7] does not propose any detailed procedures in this respect including the case of solutions. In this section, the photoprotection of *Fluvo* with excipient dyes was assessed by Φ–order kinetics.

For this purpose, the UV–absorbing food additive/excipient–dye *TRZ* was selected as its spectrum overlaps that of *Fluvo*, hence acting as an absorption competitor. Its effect was evaluated on solutions of *TRZ* of various concentrations, which were each irradiated after the addition of the same amount of *Fluvo*. It is worth mentioning that prior to the addition of *Fluvo*, the *TRZ* solution was considered for the blank experiment on the UV/Vis diode array spectrophotometer. In these conditions, the temporal evolution of the absorbance of the medium could be recorded without the spectral interference of the dye (the latter however does absorb part of the excitation light).

The resultant kinetic traces ($\lambda_{irr}/\lambda_{obs}$ = 280/245) were fitted with Eq.2 (Fig.6) and their respective reactions rate–constants were determined (Table 3). Indeed, Eqs.1–6 apply except that the total absorbance of the medium at the irradiation wavelength in Eq.4 must take

into account the presence of the third molecule of the light–absorption competitor, i.e. the actual photokinetic factor, $F_{\lambda_{irr}}^{E/Z,TRZ}(\infty)$, involves $A_{tot}^{\lambda_{irr}/\lambda_{irr}}(\infty) = A_{E/Z}^{\lambda_{irr}/\lambda_{irr}}(\infty) + A_{TRZ}^{\lambda_{irr}/\lambda_{irr}}$. The model equation (Eq.2) fitted well all the curves irrespective of the concentration of *TRZ* present in solution (though below the limit of its linearity range). Accordingly, the overall photoreaction rate–constant decreased with increasing *TRZ* concentration. Up to 75% photostabilization of *Fluvo* was recorded for the highest *TRZ* concentration used in this study (4.68 x 10^{-5} M, Table 3). This confirms that the presence of the excipient–dye does not alter the photodegradation pattern and or quantum yields of the photoreactions but only reduces the rate of photodegradation. As stipulated by Eq.4., the photodegradation rate reduction is solely related to a reduction in the value of the photokinetic factor ($F_{\lambda_{irr}}^{E/Z,TRZ}$) which itself is due to an effective increase of the medium absorbance at λ_{irr} $\left(A_{E/Z}^{\lambda_{irr}/\lambda_{irr}}(\infty) + A_{TRZ}^{\lambda_{irr}/\lambda_{irr}}\right)$.

Table 3: Dye absorbances, overall reaction rate–constants, photokinetic factors, and percentage reduction in reaction rates of *Fluvo* photodegradation in the presence of various concentrations of *TRZ* when irradiated at 280 nm and observed at 245 nm.

	$A_{dye}^{\lambda_{irr}}$ [a]	$F_{\infty}^{\lambda_{irr}}$	$k_{Fluvo}^{\lambda_{irr}}$ /s^{-1}	$\frac{k_{Fluvo}^{\lambda_{irr}}\left(A_{dye}^{\lambda_{irr}}=0\right)}{k_{Fluvo}^{\lambda_{irr}}\left(A_{dye}^{\lambda_{irr}}\neq 0\right)}$	% reduction [b]
Fluvo [c,d]	0	2.28	0.00087	1	0
Tartrazine (*TRZ*)	0.314	1.18	0.00051	1.71	41.4
	0.406	1.01	0.00044	1.98	49.4
	0.483	0.89	0.00037	2.32	56.9
	0.933	0.51	0.00022	3.87	74.1

[a]: Absorbance of the dye measured at the irradiation wavelength of 280 nm for concentrations given in Fig.6.
[b]: The constant concentration of *Fluvo* was 2.95 x 10^{-6} M.
[c]: The radiant power value for the experiments was P_{390} = 5.06 x 10^{-6} – 5.18 x 10^{-6} einstein.dm^{-3}.s^{-1}.
[d]: the optical path lengths: $l_{\lambda_{irr}}$= 2 cm; $l_{\lambda_{obs}}$= 1 cm

Furthermore, as predicted by Eq.3, a good linear relationship was found between $k_{A \leftrightarrows B}^{\lambda_{irr}}$ and $F_{\lambda_{irr}}^{E/Z,TRZ}$ (with intercept close to zero and a correlation coefficient close to unity) (Fig. 7). A similar phenomenon should also be expected to occur for an increase of the initial concentration of the mother compound (Eq.3), and hence, the rate of the reaction is concentration–dependent. This confirms that zero– and first–order reaction treatments and interpretation of photodegradation kinetics are neither suitable nor reliable approaches.

The present Φ–order kinetics equations offer however an easy and useful tool to evaluate photostabilisation of drugs in solution.

3.g Fluvo–Actinometer

An additional interesting and useful aspect offered by the equations of Φ–order kinetics is the development of new actinometers. This may represent an important concept because no standard procedures have yet been established for the evaluation of drugs potential for actinometry and/or the proposal of new actinometers.[5,6,40,41] Besides, the ICH adopted quinine hydrochloride actinometer holds a number of drawbacks that raised many of questions and doubts about its reliability.[5,6,10,42-44]

The assessment of *Fluvo* potential for actinometry is set out by preparing solutions of approximately the same concentration and exposing each one to a monochromatic light of given radiant power values selected from a set for each irradiation wavelength (260, 270, 280, 285 and 290 nm). The kinetic traces obtained at the observation wavelength of 245 nm were then well fitted to the model Eq. 2 (Fig.8). A linear correlation was observed between the

values of $k_{A\leftrightarrows B}^{\lambda_{irr}}$ and $P_{\lambda_{irr}}$ for each set of irradiation experiments (Table 4) as predicted by Eq.2. Our experimental $\beta_{\lambda_{irr}}$ and $\delta_{\lambda_{irr}}$ values matched well those calculated from Eqs.3 and 6.

Table 4: Correlation equations for the variation of the overall rate–constants ($k_{NIS}^{\lambda_{irr}}$) and initial reaction velocities ($v_0^{\lambda_{irr}/\lambda_{obs}}$) with radiant power ($P_{\lambda_{irr}}$), of *Fluvo* (2.95 x 10^{-6}M) photodegradation in water ($l_{\lambda_{irr}}$= 2 cm; $l_{\lambda_{obs}}$= 1 cm) together with the corresponding $\beta_{\lambda_{irr}}$ and $\delta_{\lambda_{irr}}$ factors, $F_{\lambda_{irr}}(0)$, $F_{\lambda_{irr}}(pss)$ and the span of radiant power employed for various monochromatic irradiations.

Irradiation wavelength λ_{irr} / nm	Equation of the line [a]	Correlation coefficient, r^2	$F_{\lambda_{irr}}(0)$	$F_{\lambda_{irr}}(pss)$	$P_{\lambda_{irr}} \times 10^7$ /einst.s^{-1}.dm^{-3}
	$k_{Fluvo}^{\lambda_{irr}} = \beta_{\lambda_{irr}} \times P_{\lambda_{irr}} + intercept$				
260	$818.4\times P_{260} + 3\times10^{-7}$	0.99	2.136	2.199	2.93 – 4.60
270	$1249\times P_{270} + 3\times10^{-5}$	0.96	2.194	2.244	2.50 – 5.21
280	$1584\times P_{280} - 1\times10^{-6}$	0.99	2.249	2.277	2.70 – 5.51
285	$1998\times P_{285} + 2\times10^{-5}$	0.98	2.273	2.287	2.63 – 4.81
290	$2077\times P_{290} + 5\times10^{-5}$	0.99	2.284	2.291	2.56 – 4.42
	$v_0^{\lambda_{irr}/\lambda_{obs}} = \delta_{\lambda_{irr}} \times P_{\lambda_{irr}} + intercept$				
260	- 10.58 x P_{260} + 4.8x10^{-7}	0.93	2.136	2.199	2.93 – 4.60
270	- 14.57 x P_{270} – 8.9x10^{-7}	0.98	2.194	2.244	2.50 – 5.21
280	- 25.16 x P_{280} + 1.3x10^{-6}	0.99	2.249	2.277	2.70 – 5.51
285	- 28.11 x P_{285} + 1.8x10^{-7}	0.99	2.273	2.287	2.63 – 4.81
290	- 31.08 x P_{290} + 1x10^{-6}	0.99	2.284	2.291	2.56 – 4.42

[a] $k_{Fluvo}^{\lambda_{irr}}$, $v_0^{\lambda_{irr}/\lambda_{obs}}$ and intercepts expressed in s^{-1}; $\beta_{\lambda_{irr}}$ and $\delta_{\lambda_{irr}}$ in einst^{-1}.dm^3.

The gradients of the lines (of $k_{A\leftrightarrows B}^{\lambda_{irr}}$ *vs.* $P_{\lambda_{irr}}$), the *beta* factors ($\beta_{\lambda_{irr}}$), represent constant coefficients that are independent of the light intensity for each irradiation

wavelength. Additionally, a linear correlation also exists between $\upsilon_{0\ (mod.)}^{\lambda_{irr}/\lambda_{obs}}$ and $P_{\lambda_{irr}}$ with gradients specific to each irradiation wavelength defined as the $\delta_{\lambda_{irr}}$ factors (Table 4) as derived from the initial velocity Eq.6. The linear relationships found here confirm the usefulness of *Fluvo* for actinometry.

Plotting the kinetic parameters $\beta_{\lambda_{irr}}$ and $\delta_{\lambda_{irr}}$ against irradiation wavelength, yield linear correlations, within the 260–290 nm irradiation range, as given by (Fig.9).

The procedure for *Fluvo*–actinometry is set out on two simple strategies for the determination of the radiant power of an unknown source of light ($P_{\lambda_{irr}}^{unk.}$) for the range 260–290 nm. Firstly, (a)– a fresh solution of *Z–Fluvo* (3 x 10^{-6} M in water) is subjected to a monochromatic irradiation (λ_{irr}) beam from the unknown source. (b)– The experimental kinetic trace hence obtained is fitted to Eq.2 and its $k_{A\leftrightharpoons B}^{\lambda_{irr}}$ value determined; and/or the $\upsilon_{0\ (mod.)}^{\lambda_{irr}/\lambda_{obs}}$ of the reaction is derived from the trace (Eq.5). In a third step, (c)– the corresponding values for the $\beta_{\lambda_{irr}}$ and/or $\delta_{\lambda_{irr}}$ factors are worked out from the corresponding relationships at λ_{irr} as given by the equations laid out in Fig.9. Finally, (d)– the unknown radiant power of the source is determined from one of the following equations (Eqs.17).

$$P_{\lambda_{irr}}^{unk.} = \frac{k_{A\leftrightharpoons B}^{\lambda_{irr}}}{\beta_{\lambda_{irr}}} = \frac{\nu_{0}^{\lambda_{irr}/\lambda_{obs}}}{\delta_{\lambda_{irr}}} \qquad (17a,b)$$

In order to facilitate even more the actinometric method, the $\nu_{0,Cld.}^{\lambda_{irr}/\lambda_{obs}}$ values calculated using Eq.6 were compared to those ($\nu_{0,Exp.}^{\lambda_{irr}/\lambda_{obs}}$) obtained as the gradient of the

linear fit of the data corresponding to the early stages of the reaction (Fig.10). A very good agreement has been found, indicating that the initial velocity values can be worked out from the data corresponding to the first 5 to 10 min of *Fluvo* irradiation. This finding makes the development of AB(2Φ) actinometers a less time–consuming process, which would be decisive for very slow reactions.

Nevertheless, if the concentration or path–lengths used in the unknown light source experiment differ from the ones employed in this study (i.e. 2.95 x 10^{-6} M and $l_{\lambda_{irr}}$ = 2 cm, respectively), then the $\beta_{\lambda_{irr}}$must first be adjusted before being substituted in Eq.17a. This can be achieved by dividing the $\beta_{\lambda_{irr}}$ value obtained in step (c) of the procedure above by $2 \times F_{\lambda_{irr}}(pss)$ (the latter corresponding to our experiment) and then multiplying it by the value of the new path–length and the photokinetic factor corresponding to the path–length and concentration used in the unknown light source experiment. Similarly, a correction is also needed for $v_0^{\lambda_{irr}/\lambda_{obs}}$ if different path-lengths and/or initial concentration were used. This can be achieved by dividing $v_0^{\lambda_{irr}/\lambda_{obs}}$ by $2 \times F_{\lambda_{irr}}(0)$ and then multiplying it by the values of the new path–length and initial photokinetic factor used.

As well as facilitating actinometry studies, the $\beta_{\lambda_{irr}}$can also serve to inform about a photoreaction rate much more reliably than the overall rate–constant or the quantum yields. Unlike $k_{A \leftrightharpoons B}^{\lambda_{irr}}$ and $\Phi^{\lambda_{irr}}$, $\beta_{\lambda_{irr}}$offers the possibility of comparing the rates of photoreactions within the same or different experimental settings employing the same initial concentrations. This is because $\beta_{\lambda_{irr}}$ takes into account all photoreaction attributes and experimental parameters at the exception of the radiant power (which is hardly replicable – between experiments). This parameter is, therefore, an ideal tool for comparing the photoreaction rates between different experiments and we propose to label it as the "*pseudo–rate–constant*".

(Similarly, $\delta_{\lambda_{irr}}$ could be considered as a *pseudo-initial velocity* varying only with the terms given in Eq.6 but not with radiant power.) For instance, the wavelength causative range for *Fluvo* photodegradation is clearly situated above λ_{irr}= 280 nm, with $\beta_{\lambda_{irr}}^{Fluvo} > 1500$ einst^{-1}.dm^{3}. However, if the wavelength range was overlooked, the photodegradation of *Fluvo* is 10 to 20 times slower than that of Montelukast with $1.7 \times 10^4 > \beta_{\lambda_{irr}}^{Monte} > 2.8 \times 10^4$ (despite $\Phi_{A\rightarrow B,Fluvo}^{\lambda_{irr}} > \Phi_{A\rightarrow B,Monte}^{\lambda_{irr}}$).[12] Therefore, this parameter opens new perspectives in comparing photoreactions' rates, which have long been awaited, since it is well documented that the (0^{th}–, 1^{st}–, or 2^{nd}–order) overall rate–constant (k) cannot be used comparatively between different experimental settings using the same or different photoreactive species.[5] The quantum yield, on the other hand, informs specifically on the inherent efficiency of a molecule to photoreact in a particular solvent under a given irradiation wavelength, which would be proportional to the reaction rate if and only if the reactive species is the only compound absorbing the excitation light (Eq.3).[8,10] However, the quantum yield value does not give a full picture on the photoreaction rate if there are more than one species absorbing irradiation in the medium and/or many photochemical steps are involved in the phototransformation mechanism.

4. Conclusion

The above study emphasises the new perspectives offered by the Φ–order kinetic model for photoreversible systems in general. For the particular case of drugs, it sets out a framework for targeted, accurate and complete kinetic studies. Φ–order kinetic then represents a more efficient tool for the assessment and quantification of both photosatbility and photostabilisation of drugs than the classical treatment based on 0^{th}–, 1^{st}– and 2^{nd}–order kinetics. It can serve the development of new technological AB(2Φ) devices in photomedicine, targeted drug delivery and photo–responsive drug nano–carrier systems.[45-48] The data provided by such studies may also be of importance for photosafety studies and might be recommended prior to conducting the evermore required *in vivo* safety studies.

Using *Fluvo* as an example of photoreversible reaction systems, the model (i)– fitted its full kinetic traces; (ii)– allowed the determination of the overall–rate constant; (iii)– offered the pseudo–rate–constant beta factors as a new and reliable kinetic parameter truly reflective of intra– and inter–experiments' rate of photoreactions; (iv)– allowed the quatification of effects of photostabilising additives; and (v)– presented *Fluvo* as an accurate and reliable actinometer for the 260–290 nm irradiation range.

REFERENCES

1. Koheler, J.M. In Drug-Induced Diseases: Prevention, detection and management (Eds: J.E. Tisdale, D.A. Miller), Hearthside Publishing. Bethesda, pp. 117-134, 2010.

2. Bjertness, E. Solar Radiation and Human Health. The Norwegian Academy of Science and Letters, Oslo, pp:102-113, 2008.

3. Ferguson, J. Investigation of drug-induced photosensitivity in man. *Toxicology.* **226**, 25-26, 2006.

4. Ferguson, J. In *Photodermatology* (Eds: J. Ferguson, J.S. Dover)**.** Photodermatology. Manon Publishing Ltd. London, 2006.

5. Piechocki, J.T. and K. Thoma, Pharmaceutical Photostability and Photostabilisation Technology. Informa Healthcare, London, 2010.

6. Tonnesen, H.H. Photostability of Drugs and Drug Formulations (second Edition). CRC Press: London, 2004.

7. ICH, Guidance for industry Q1B photostability testing of new drug substances and products, *Fed. Regist.* **62**, 27115-27112, 1996.

8. Maafi, M. and R.G. Brown, The kinetic model for AB(1Φ) systems: A closed-form integration of the differential equation with a variable photokinetic factor. *J. Photochem. Photobiol. A: Chem.,* **187**, 319-324, 2007.

9. Maafi, M. and R. Brown, Kinetic analysis and kinetic elucidation options for AB(1k,2Φ) systems. New Spectrokinetic methods for photochromes. *Photochem. Photobiol. Sci.,* **7**, 1360 – 1372, 2008.

10. Maafi, W. and M. Maafi, Modelling Nifedipine Photodegradation, Photostability and Actinometric Properties. *Int. J. Pharm.,* **456**, 153–164, 2013.

11. Maafi, M. and W. Maafi, Φ-order kinetics of photoreversible drug reactions. *Int. J. Pharm*., **471**, 536–543, 2014.

12. Maafi, M. and W. Maafi, Montelukast photodegradation: Elucidation of Φ-order kinetics, determination of quantum yields and application to actinometry. *Int. J. Pharm.***, 471**, 544–552, 2014.

13. Fukui, N., Y. Suzuki, T. Sugai, J. Watanabe, S. Ono, N. Tsuneyama and T. Someya, Promoter variation in the catechol-*O*-methyltransferase gene is associated with remission of symptoms during fluvoxamine treatment for major depression. *Psych. Res.*, **218**, 353–355, 2014.

14. Figgitt, D.P. and K.J. McClellan, Fluvoxamine: An updated review of its use in the management of adults with anxiety disorders. *Drugs.* **60**, 925-954, 2000.

15. Benfield, P. and A. Ward, Fluvoxamine: a review of its pharmacodynamics and pharmacokinetic properties, and therapeutic efficacy in depression illness. *Drugs*. **32**, 313–334, 1986.

16. Honda, M., K. Uchida, M. Tanabe and H. Ono, Fluvoxamine, a selective serotonin reuptake inhibitor, exerts its antiallodynic effects on neuropathic pain in mice via 5-HT2A/2C receptors. *Neuropharmacology.* **51**, 866-872, 2006.

17. Velasco, A., C. Alamo, J. Heras and A. Carvajal, Effects of fluoxetine hydrochloride and fluvoxamine maleate on different prepaprations of isolated guinea-pig and rat organ-tissues. *Gen. Pharmacol.* **28**, 509-512, 1997.

18. Muck-Seler, D., N. Pivac and M. Diksic, Acute treatment with fluvoxamine elevates rat brain serotonin synthesis in some terminal regions: an autoradiographic study. *Nucl. Med. Biol.,* **39**, 1053-1057, 2012.

19. Panahia, H.A., Y.T.E. Monirib and E. Keshmirizadeh, Synthesis and characterization of poly[*N*-isopropylacrylamide-*co*-1-(*N*,*N*-*bis*-carboxymethyl)amino-3-allylglycerol] grafted to magnetic nano-particles for the extraction and determination of fluvoxamine in biological and pharmaceutical samples. *J. Chromatogr. A.,* **1345**, 37–42, 2014.

20. Miolo, G., S. Caffieri, L. Levorato, M. Imbesi , P. Giusti, T. Uz, R. Manev and H. Manev, Photoisomerization of fluvoxamine generates an isomer that has reduced activity on the 5-hydroxytryptamine transporter and does not affect cell proliferation. *Eur. J. Pharmacol.*, **450**, 223– 229, 2002.

21. Kwon, J.W. and K.L. Armbrust, Photo-isomerization of fluvoxamine in aqueous solutions. *J. Pharm. Biomed. Anal.,* **37**, 643–648, 2005.

674 22. Iijima, K., M. Suzuki, T. Sakaizumi and O. Ohashi, Molecular structure of gaseous
675 acetoxime determined by electron diffraction. *J. Mol. Struct.,* **413-414**, 327-331,
676 1997.

677 23. Black, M. and K. Armbrust, 2007. Final Report: The Environmental Occurrence,
678 Fate, and Ecotoxicity of Selective Serotonin Reuptake Inhibitors (SSRIs) in Aquatic
679 Environments. Available at:
680 http://cfpub.epa.gov/ncer_abstracts/index.cfm/fuseaction/display.abstractDetail
681 /abstract/1755/report/F. Accessed on 3 January 2015.

682 24. Maafi, M. The potential of AB(1Φ) systems for direct actinometry. Diarylethenes as
683 successful actimometers for the visible range. *Phys. Chem. Chem. Phys*., **12**, 13248–
684 13254, 2010.

685 25. Maafi, M. and R. Brown, General analytical solutions for the kinetics of AB(k,Φ) and
686 ABC(k,Φ) systems. *Int. J. Chem. Kinet*., **37**, 162 – 174, 2005.

687 26. Maafi, M. and R. Brown, Analysis of diarylnaphthopyran kinetics. Degeneracy of the
688 kinetic solution*. Int. J. Chem. Kinet.,* **37**, 717 – 727, 2005.

689 27. Gilbert, A., J. Bagott, Essentials of molecular photochemistry. Blackwell Science.
690 Oxford, 1991.

691 28. Neckers, D.C., D.H. Volman and G. Von Bunau, Advances in photochemistry, vol.
692 19. John Wiley & Sons, New York, 1995.

693 29. Singh, J. Photochemistry and pericyclic reactions. New Age International, New Delhi,
694 2005.

695 30. Kutlubay, Z., A. Sevim, B. Engin and Y. Tuzun, Photodermatoses, including
696 phototoxic and photoallergic reactions (internal and external). *Clin. Dermatol.*, **32**,
697 73–79, 2004.

698 31. Arnold, A., C. Pedroza and E. Tyson, Phototherapy in ELBW newborns: Does it
699 work? Is it safe? The evidence from randomized clinical trials. *Semin. Perinatol.,* **38**,
700 452–464, 2014.

701 32. Feldmeyer, L., G. Shojaati, K.S. Spanaus, A. Navarini, B. Theler, D. Donghi, M.
702 Urosevic-Maiwald, M. Glatz, L. Imhof, M.J. Barysch, R. Dummer, M. Roos, L.E.

French, C. Surber and G.F.L. Hofbauer, Phototherapy with UVB narrowband, UVA/UVBnb, and UVA1 differentially impacts serum 25-hydroxyvitamin-D3. *J. Am. Acad. Dermatol.*, **69**, 530–536, 2013.

33. Drucker, A.M. and A.M.C.F. Rosen, Drug-induced photosensitivity: culprit drugs, management and prevention. *Drug Saf.* **34**, 821–837, 2011.

34. ICH(S10), 2013. ICH Harmonised Tripartite Guideline Photosafety Evaluation of Pharmaceuticals S10. Available at: http://www.ich.org/fileadmin/Public_Web_Site/ICH_Products/Guidelines/Safety/S10/S10_ Step_4.pdf . Accessed on 3 January 2015**.**

35. FDA Food and Drug Administration Center for Drug Evaluation and Research (CDER), 2003. Guidance for Industry: Photosafety Testing. Available at: http://www.fda.gov/cder/guidance/index.htm. Accessed on 3 January 2015.

36. The European Agency for the Evaluation of Medicinal Products (EMEA), 2002. Committee for Proprietary Medicinal Products (CPMP)**.** Note for guidance on photosafety testing. CPMP/SWP/398/01. Available at: http://www.emea.eu.int/. Accessed on 3 January 2015.

37. Krul, C., W. Maas, R. Van Meeuwen, N. De Vogel and M.J. Steenwinkel, In vivo photogenotoxicity testing, bridging the gap between in vitro photogenotoxicity and photocarcinogenicity testing. *Toxicology*. **226**, 1-25, 2006.

38. Cameron, H., S. Yule, R.S. Dawe, H. Ibbotson, H. Moseley and J. Ferguson, Review of an established UK home phototherapy service 1998-2011: improving access to a cost-effective treatment for chronic skin disease. *Public Health.* **128**, 317–324, 2014.

39. Gambichler, T., S. Terras and A. Kreuter, Treatment regimens, protocols, dosage, and indications for UVA1 phototherapy: facts and controversies. *Clin. Dermat.,* **31**, 438-454, 2013.

40. Kuhn, H.J., S.E. Braslavsky and R. Schmidt, Chemical actinometry (IUPAC Technical Report). *Pure appl. Chem.*, **76**, 2105-2146, 2004.

41. Montali, M., A. Credi, L. Prodi and M.T. Gandolfi, Handbook of photochemistry (3rd Ed.). CRC Press – Taylor & Francis, Boca Raton-London-New York, 2006.

42. Baertschi, S.W. Commentary on the quinine actinometry system described in the ICH draft guideline on photostability testing of new drug substances and products. *Drug Stab.,* **1**, 193–195, 1997.

43. Baertschi, S.W., K.M. Alsante and H.H. Tonnesen, A critical assessment of the ICH guideline on photostability testing of new drug substances and products (Q1B): recommendation for revision. *J. Pharm. Sci.,* **99**, 2934–2940, 2010.

44. De Azevedo Filho, C.A., D. De Filgueiras Gomes, J.P. De Melo Guedes, R. M. F. Batista and B.S. Santos, Considerations on the quinine actinometry calibration method used in photostability testing of pharmaceuticals. *J. Pharm. Biomed. Anal*. **54**, 886–888, 2011.

45. Wohl, B.M. and J.F.J. Engebersen, Responsive layer-by-layer materials for drug delivery. *J. Control.Release*. **158**, 2-14, 2012.

46. Tomatsu, I., K. Peng and A. Kros, Photoresponsive hydrogels for biomedical applications. *Adv.Drug Del.Rev*. **63**, 1257-1266, 2011.

47. Fomina, N., J. Sankaranarayanan and A. Almutairi, Photochemical mechanisms of light-triggered release from nanocarriers. *Adv. Drug Del. Rev*. **64**, 1005-1020, 2012.

48. Feliciano, M., D. Vylta, K.A. Medeiros and J.J. Chambers, The $GABA_A$ receptor as a target for photochromic molecules. *Bioorg. Med. Chem*., **18**, 7731-7738, 2010.

Figures

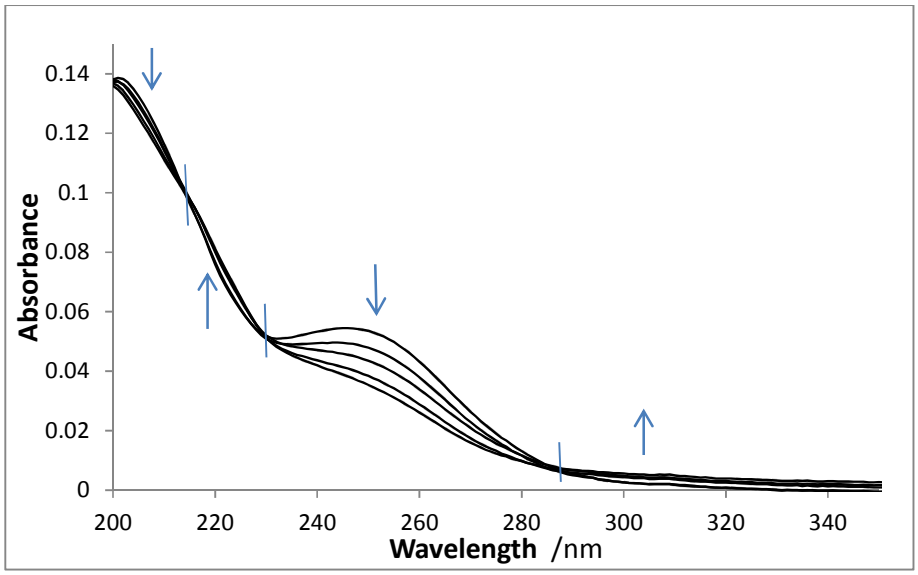

Fig. 1. Evolution of the electronic absorption spectra of 4.01 x 10^{-6} M *Fluvo* in water subjected to steady state irradiation with a 270–nm monochromatic beam (total irradiation time 26 min at a radiant power of P_{270} = 7.37 x 10^{-7} einstein.s^{-1}.dm^{-3}). The arrows indicate the direction of the absorbance evolution during the photoreaction and the vertical lines cross the spectra at the isosbestic points (215, 226, 285 nm).

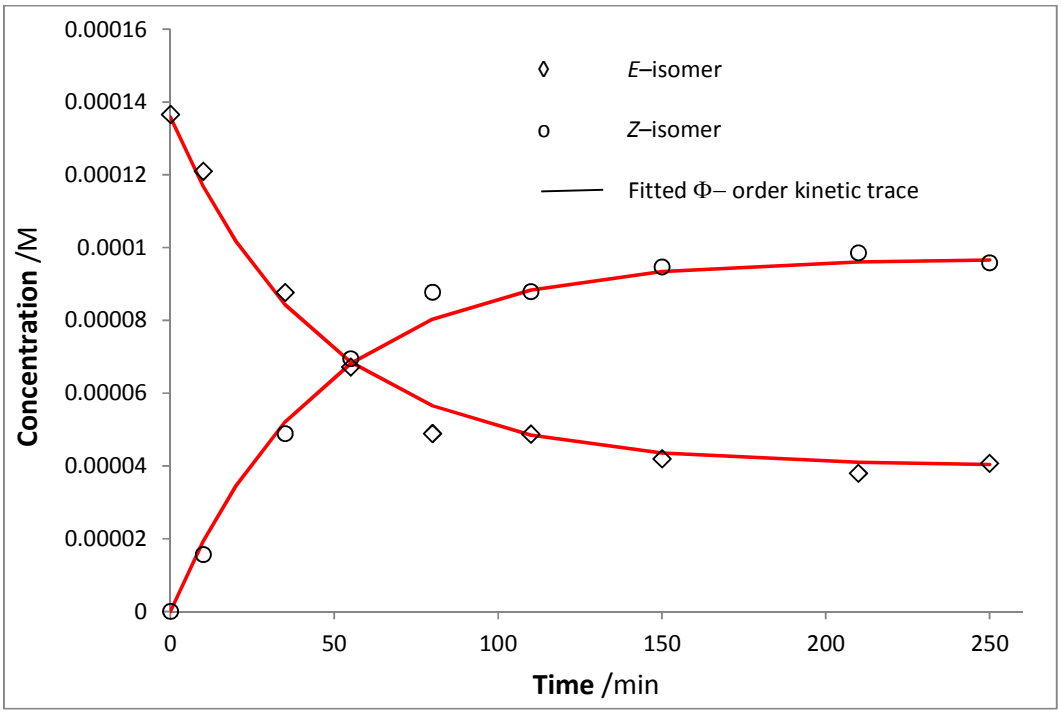

Fig. 2: Change in aqueous *E–Fluvo* solution (1.37 x 10^{-4} M) and its *Z*–isomer photoproduct concentrations over 5 hours upon exposure to an isosbestic monochromatic irradiation of 226 nm (P_{226}= 1.88 x 10^{-6} einstein.s^{-1}.dm^{-3}) as monitored by HPLC.

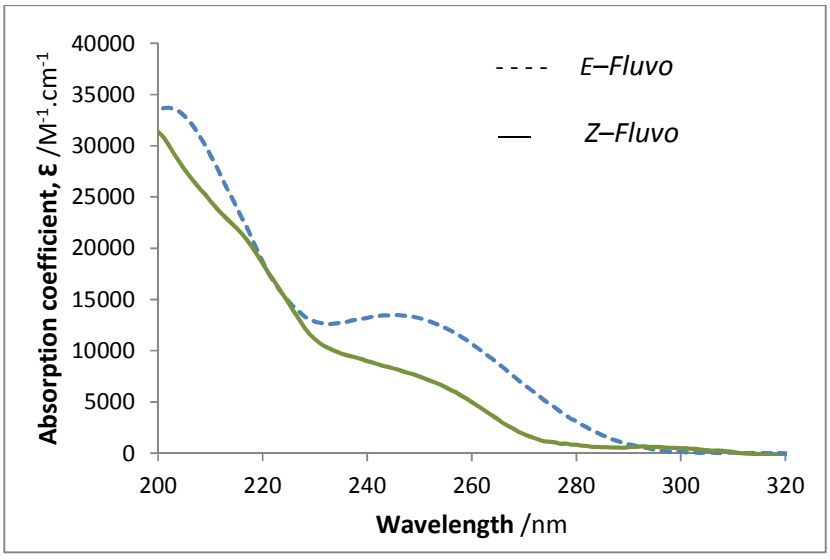

Fig. 3. Electronic absorption spectra (absorption coefficient units) of *E*– (native) and *Z–Fluvo (recovered).*

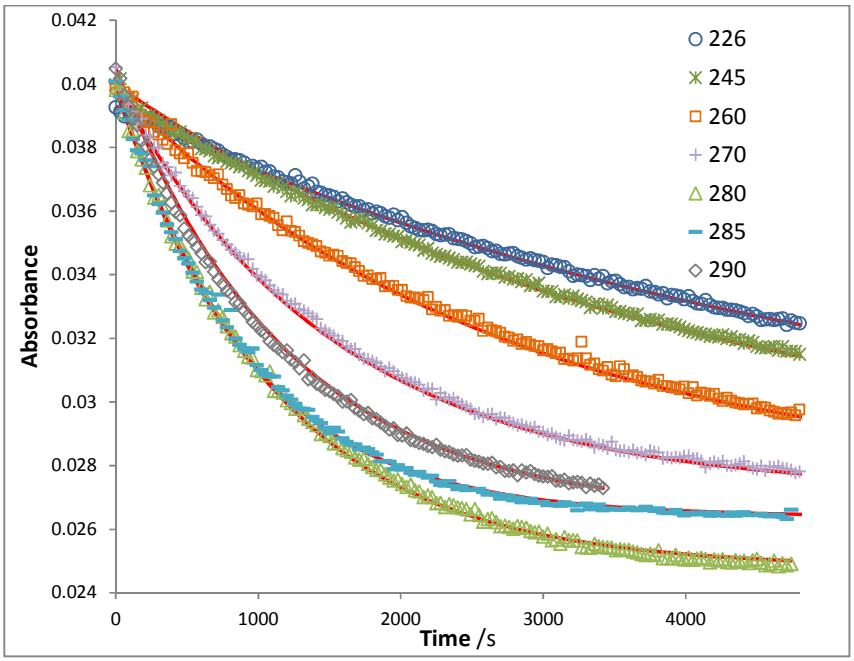

Fig. 4. The photokinetic traces of *Fluvo* photodegradation in water (2.95 x 10^{-6} M) at λ_{irr} = 226, 245, 260, 270, 280, 285 and 290nm and observed at λ_{obs}= 245nm. The geometric shapes represent the experimental data while the continuous lines represent the model fitted traces using the appropriate model equation.

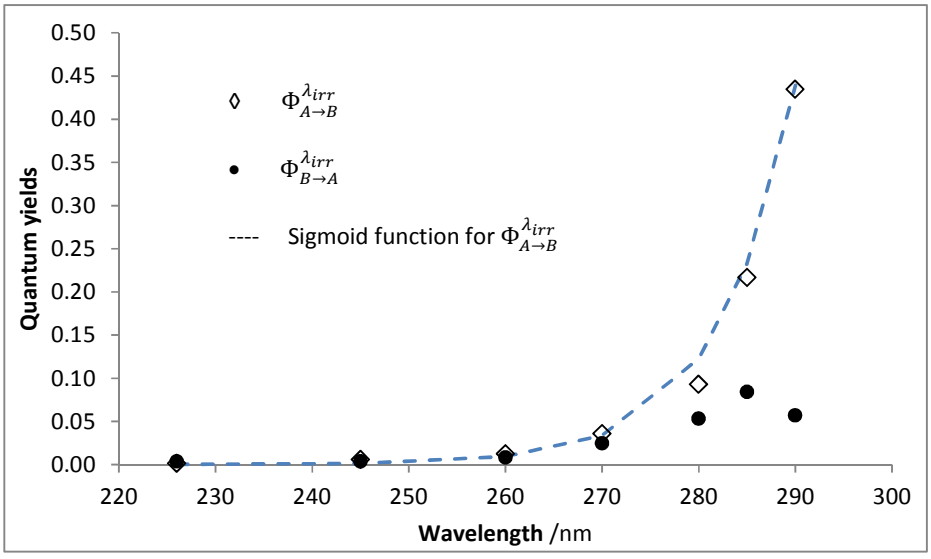

Fig. 5: Average forward ($\Phi_{A\to B}^{\lambda_{irr}}$) (diamonds) and reverse ($\Phi_{B\to A}^{\lambda_{irr}}$) (plain circles) *Fluvo* quantum yields for irradiation wavelengths 226, 245, 260, 270, 280, 285 and 290 nm.

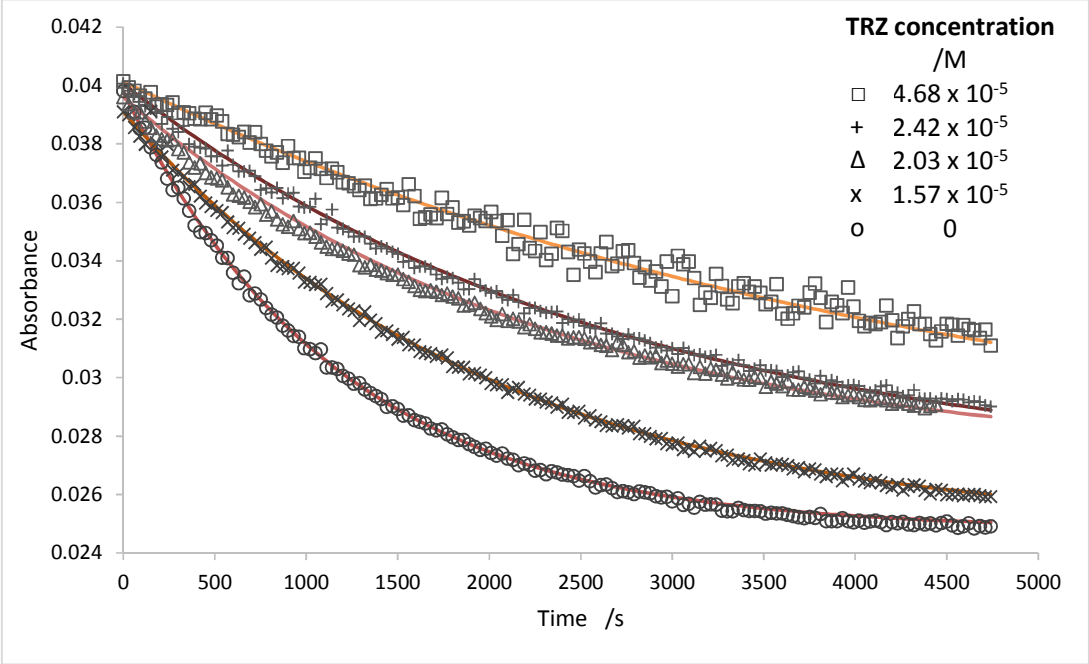

Fig. 6: Effect of increasing *TRZ* concentrations on the photodegradation traces of 2.95 x 10^{-6} M aqueous *Fluvo* solutions when irradiated at 280 nm and observed at 245 nm.

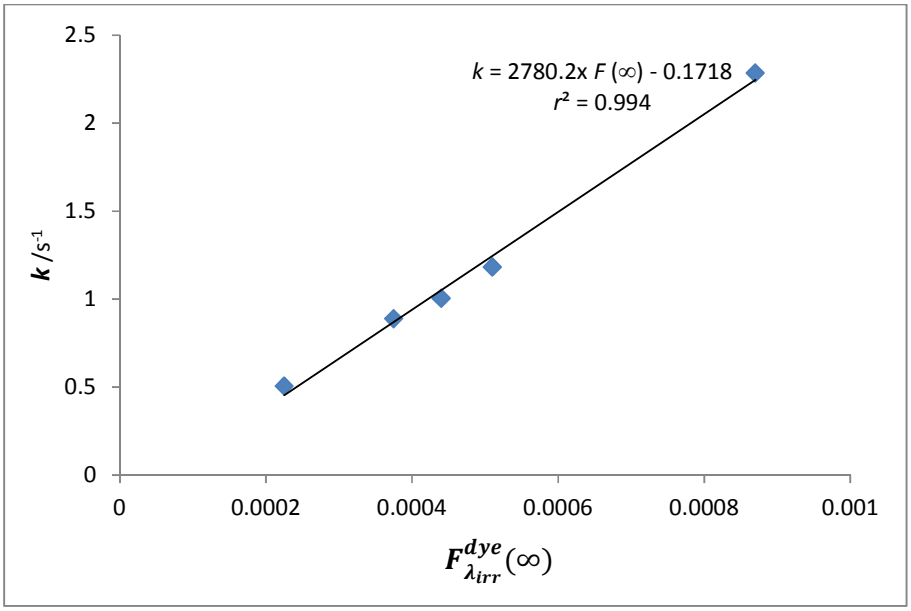

Fig. 7: Linear relationship between *Fluvo* overall rate–constant of photodegradation in the presence of increasing concentrations of *TRZ* with the corresponding photokinetic factors ($F^{dye}_{\lambda_{irr}}(\infty)$).

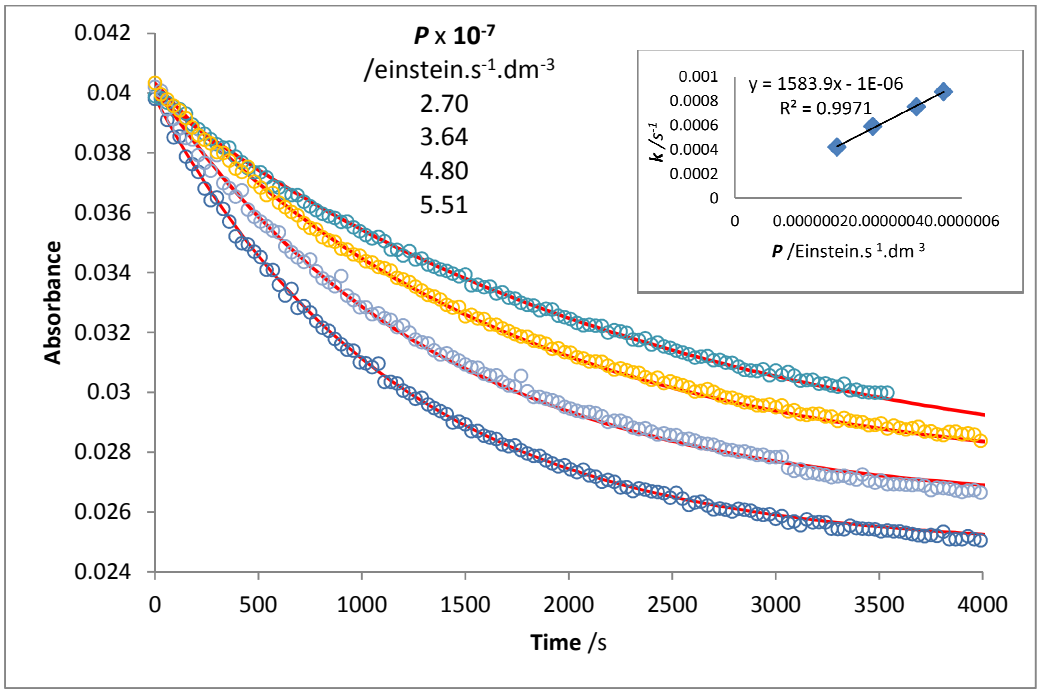

Fig. 8. Effect of increasing the irradiation radiant power ($P_{\lambda_{irr}}$) on the kinetic traces of *Fluvo* (2.97 x 10^{-6} M) when irradiated at 280 nm and observed at 245 nm. The circles represent the experimental data while the lines represent the model fitted traces.

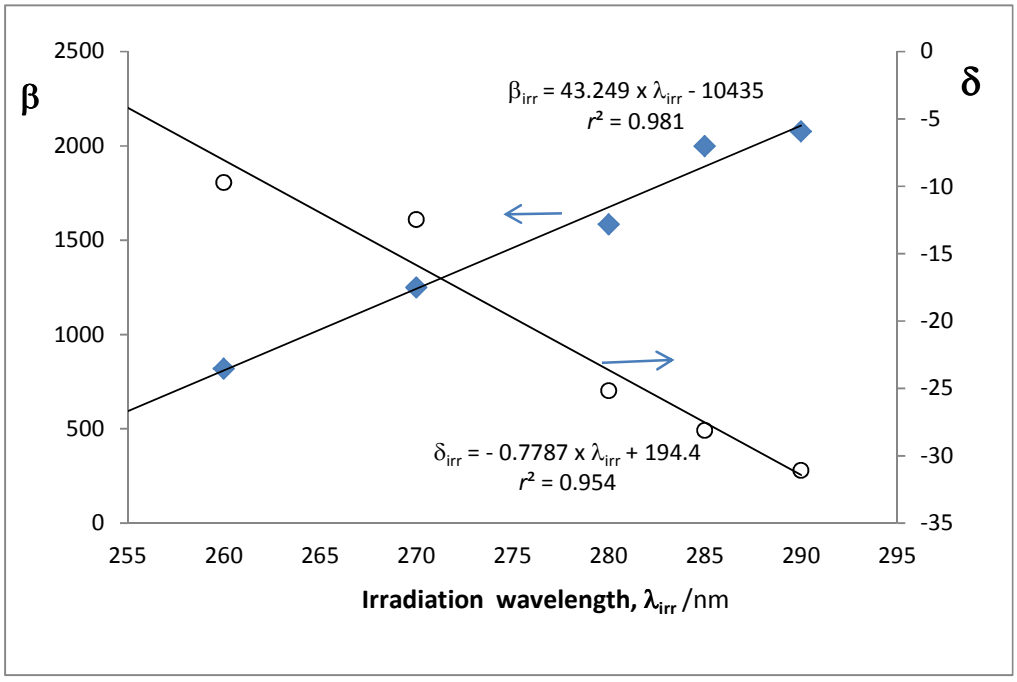

Fig. 9: Linear correlation between $\beta_{\lambda_{irr}}$ and $\delta_{\lambda_{irr}}$ with irradiation wavelength.

$\beta_{\lambda_{irr}}$ and $\delta_{\lambda_{irr}}$ in einst^{-1}.dm^{3}.

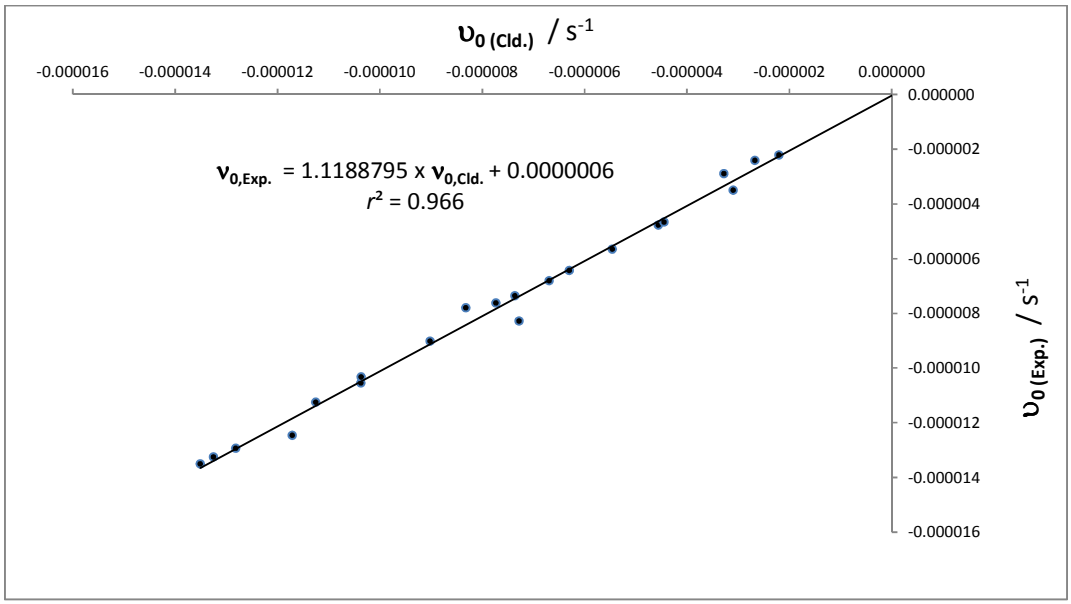

Fig. 10: Correlation between $\nu_{0(Cld.)}^{\lambda_{irr}/\lambda_{obs}}$ and $\nu_{0(Exp.)}^{\lambda_{irr}/\lambda_{obs}}$ for all the sets of *Fluvo* actinometry experiments in Table 4.